Available online at www.sciencedirect.com
ScienceDirect
Journal of Membrane Science 293 (2007) 167–173
journal of MEMBRANE SCIENCE
www.elsevier.com/locate/memsci

Modeling transient permeation of polar organic mixtures through a MFI zeolite membrane using the Maxwell–Stefan equations

Miao Yu[a], John L. Falconer[a,*], Richard D. Noble[a], R. Krishna[b]

[a] *Department of Chemical and Biological Engineering, University of Colorado, Boulder, CO 80309-0424, USA*
[b] *Van't Hoff Institute for Molecular Sciences, University of Amsterdam, Nieuwe Achtergracht 166, 1018 WV Amsterdam, The Netherlands*

Received 15 December 2006; received in revised form 7 February 2007; accepted 9 February 2007

Abstract

Isotopic transient permeation of methanol/ethanol, methanol/2-propanol, and methanol/acetone mixtures through a MFI zeolite membrane was investigated experimentally. For the methanol/2-propanol and methanol/ethanol mixtures, the more mobile species (methanol) was slowed down in the mixture and the tardy species (2-propanol or ethanol) was speeded up. The extent of slowing down and speeding up depended on the mixture composition. The Maxwell–Stefan (M–S) diffusion equations reproduced the observed mixture permeation results, at least qualitatively, provided the self-exchange coefficient $Đ_{ii}$ for each species was taken to be a tenth of the pure component M–S diffusivity $Đ_i$. For the methanol/acetone mixtures, *both* species slowed down in the mixture. Adjusting the value of the self-exchange coefficient $Đ_{ii}$ in the M–S equations did not provide an explanation of the observed experimental results; it appeared that the component diffusivities, $Đ_1$ and $Đ_2$, in the mixture were both lower than the values of the pure components, an effect that has not earlier been reported in the literature.

Keywords: Zeolite membrane; Maxwell–Stefan; MFI; Transient permeation; Mixture

1. Introduction

Zeolites are aluminosilicate with molecular-sized pores, 0.3–1.3 nm. Molecules with sub-nanometer-size difference can have significantly different diffusivities in the uniform, molecular-sized pores of zeolites [1]. Zeolite membranes can take advantage of these diffusion differences, combining with adsorption differences, to separate mixtures with high efficiency [2–9]. Understanding mixture diffusion in zeolites, therefore, is important for zeolite membrane-based separation.

Molecular simulations [10] and M–S modeling [11] have been used to describe multicomponent diffusion through zeolite pores. These models indicate that slower molecules inhibit diffusion of faster molecules, whereas the slower moving molecules are either almost unaffected, even at high loading of faster moving molecules [10], or slightly sped up in some mixtures [11–13]. Desorption under reduced pressure (DRP) [14] measurements showed that for diffusion of *n*-paraffin and aromatics mixtures in MFI zeolite, fast diffusing molecules were strongly affected by the slow diffusing molecules, while the diffusivities of the slow molecules were not affected by the co-existence of fast molecules. These studies indicated that the slowing-down effect is more significant than speeding-up effect. Therefore, the correlation effect is more weighed on slower diffusing molecules.

Diffusion of mixtures with strong molecular interactions has been studied in polymeric membranes [15,16], although few such studies were done on zeolite membranes [17,18]. Plessis et al. [15] studied the permeation of a series of structurally related compounds through a PDMS membrane saturated with toluene and octanol. They found that fluxes of phenol, salicylic acid, benzoic acid, anisole, phenylethanol, and benzyl alcohol were lower in octanol-saturated PDMS membrane due to their lower diffusion coefficients, as measured by ATR-FTIR technique. They attributed this lower diffusivity to the retardation by a polar/H-bonding interaction.

Diffusion through MFI (~0.55 nm XRD pore diameter) zeolite membranes was studied in this paper because of their appropriate pore openings for many industrially important organic molecules, besides many common advantages as other zeolites, such as high thermal/hydrothermal stability, and hydrophobic/

---

* Corresponding author. Tel.: +1 303 492 8005; fax: +1 303 492 4341.
E-mail address: john.falconer@colorado.edu (J.L. Falconer).

0376-7388/$ – see front matter
doi:10.1016/j.memsci.2007.02.015

organophilic adsorption properties. Polar organic mixtures, methanol/ethanol, methanol/2-propanol, and methanol/acetone, were chosen in order to investigate the effect of strong molecular interaction on mixture diffusion in zeolites, and also because polar organic mixtures are normally separated by pervaporation with zeolite membranes [8,19–21].

2. Experimental methods

2.1. Membrane preparation and characterization

The Ge-substituted ZSM-5 membrane (M1) was prepared by *in situ* crystallization onto the inside surface of a tubular porous support (stainless steel, 0.8-μm diameter pores, Pall Corp). The synthesis gel molar composition was 0.78 $Ge(C_2H_5O)_4$: 19.5 SiO_2: 1 TPAOH: 438 H_2O: 75 2-propanol. Ludox AS 40 (silica sol) was the Si source, TPAOH (tetra-propyl ammonium hydroxide) was the template, and 2-propanol was a solvent. More details on membrane preparation have been published previously [17]. A second membrane (M2), prepared by the same method on a different support (stainless steel, 0.5-μm pores, Mott Corporation), was analyzed by SEM and electron probe microanalysis (EPMA) to determine its thickness and Si/Ge ratio. After synthesis, the membranes were calcined at 753 K for 8 h. The heating and cooling rates were 0.8 and 0.9 K/min, respectively.

Membrane M1 was used for isotopic-transient experiments. It was characterized by $n\text{-}C_4H_{10}$ and $i\text{-}C_4H_{10}$ single gas permeation at 473 K with the feed gas at 223 kPa. No sweep gas was used, and the permeate pressure was 85 kPa. Permeances of 50/50 $n\text{-}C_4H_{10}/i\text{-}C_4H_{10}$ mixtures were also measured at 300, 373, and 473 K, using feed and permeate pressures of 216 and 85 kPa, respectively. Log-mean pressure differences were used as the driving force when calculating mixture permselectivities.

2.2. Pervaporation

The apparatus used for isotopic-transient pervaporation is similar to the system described previously [17]. The membrane tube was sealed in a stainless steel module using Teflon o-rings. A centrifugal pump recirculated liquid feed through the inside of the membrane tube from a feed reservoir at approximately 1 L/min to minimize concentration polarization. The total feed volume was 40 mL. A magnetic stir bar also mixed the feed in the reservoir, which contained less than 5 mL of liquid. The feed and membrane were insulated and heated with heating tape. A thermocouple measured feed temperature, and a temperature controller was used to stabilize the feed temperature. The permeate side pressure was kept below 10 Pa using a LN_2 trap and a mechanical vacuum pump. Partial pressures in the permeate were measured with a quadrupole mass spectrometer (Pfeiffer Vacuum Prisma) through 1.6-mm stainless steel tubing. The permeate line, the 1.6-mm tubing, and the mass spectrometer chamber were heated to 380 K to minimize adsorption on the walls. To measure the system time delay, a solid tube with a 30-μm diameter pinhole was placed in the membrane module. At 303 K, flow rates through the membrane and pinhole were similar. For the solid tube, isotopically labeled methanol and acetone took about 3 s to appear in the permeate, and 7 and 12 s, respectively, to reach 97% of their steady-state values. These system response times are much smaller than the membrane response times. Increasing the stirring rate in the reservoir or the circulation pumping speed did not change the system response times. If the tubing and mass spectrometer chamber walls were not heated, the system responses were as long as several minutes.

Transient isotope permeation measurements were carried out, after the permeation rates of the unlabeled molecules were at steady state, by adding isotopically labeled molecules to the feed and monitoring their mass signals with a mass spectrometer. Steady-state fluxes were measured by collecting permeate vapors in the LN_2 trap for 2–4 h, and mixture permeate concentrations were measured by analyzing the permeate liquid with a GC. Isotopically labeled species, at the same temperature as the feed, were quickly added to the feed reservoir with a syringe. For mixtures, feed samples for GC analysis were taken just prior to isotope addition, and the isotope mixtures had the same molar concentrations as the feed, so that permeation remained at steady state.

After isotope addition, about 1% of each species in the feed was labeled, although different concentration steps, including changing from 0 to 0.4% labeled species in the feed, and from 18 to 32% labeled species, yielded the same response times. Deuterium labeling used deuterium atoms on carbon atoms because hydrogen on oxygen atoms readily exchange with each other. The parent mass signals for the isotopes were monitored when possible, but the signal-to-noise ratios were higher for some cracking fractions that were unique to the corresponding isotopes. Normalized responses of these cracking fractions overlapped with those of the parent masses. Normalized responses are presented since the responses do not depend on the amount of isotope added [17].

3. Theory

The Maxwell–Stefan (M–S) diffusion formulation [22,23]:

$$-\rho\frac{\theta_i}{RT}\nabla\mu_i=\sum_{\substack{j=1\\ j\neq i}}^{n}\frac{q_jN_i-q_iN_j}{q_{i,\text{sat}}q_{j,\text{sat}}Đ_{ij}}+\frac{N_i}{q_{i,\text{sat}}Đ_i};\quad i=1,\ldots,n \tag{1}$$

is widely used in practice for predicting *mixture* permeation across zeolite membranes. In Eq. (1) N_i is the flux of species i expressed in mol m^{-2} s^{-1}, ρ the zeolite framework density expressed as kg m^{-3}, q_i the loading of species i in a mixture in mol kg^{-1}, $q_{i,\text{sat}}$ represents the saturation loading of species i, n the total number of diffusing species, R the gas constant, and T is the absolute temperature. The fractional occupancy of component i, θ_i, is defined as

$$\theta_i=\frac{q_i}{q_{i,\text{sat}}} \tag{2}$$

Eq. (1) *defines* two types of M–S diffusivities: $Đ_i$ and $Đ_{ij}$. If we have only a single sorbed component, then only one $Đ_i$ is needed, and in this case $Đ_i$ is equivalent to the single component “corrected” diffusivity. Strictly speaking, there is no prescription in the M–S formulation about the values of the $Đ_i$, nor on the dependence of $Đ_i$ on the mixture composition and loading. The $Đ_i$ value in the mixture is commonly assumed to have the *same* value as that of the pure component i, taken at the same total occupancy:

$$\theta = \sum_{i=1}^{n} \frac{q_i}{q_{i,\text{sat}}} \tag{3}$$

The binary exchange coefficients $Đ_{ij}$ reflect *correlation* effects in mixture diffusion [24]; the $Đ_{ij}$ tends to slow down the more-mobile species and speed up the relatively tardy ones. A lower value of the exchange coefficient $Đ_{ij}$ implies a *stronger* correlation effect. When $Đ_{ij} \to \infty$, correlation effects vanish.

For *quantitative* modeling of mixture permeation, it is necessary to have a good estimation of the binary exchange parameter $Đ_{ij}$. In early work [23] a procedure for estimating this exchange parameter from the M–S diffusivities of the pure components,

Methanol –2-propanol mixtures

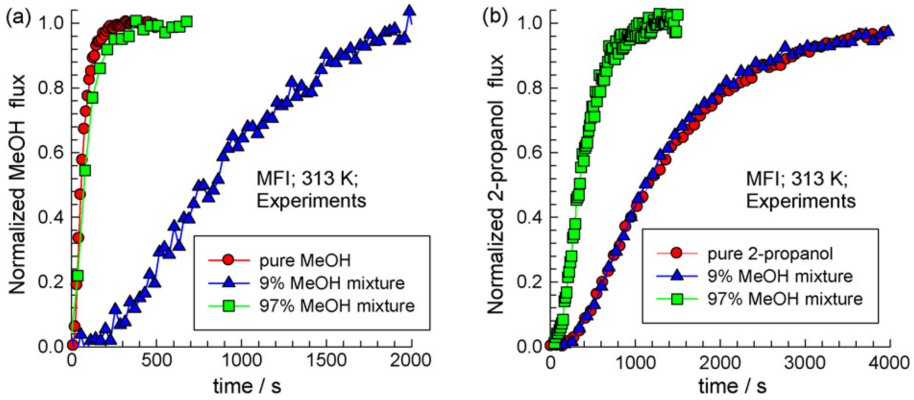

Methanol – ethanol mixtures

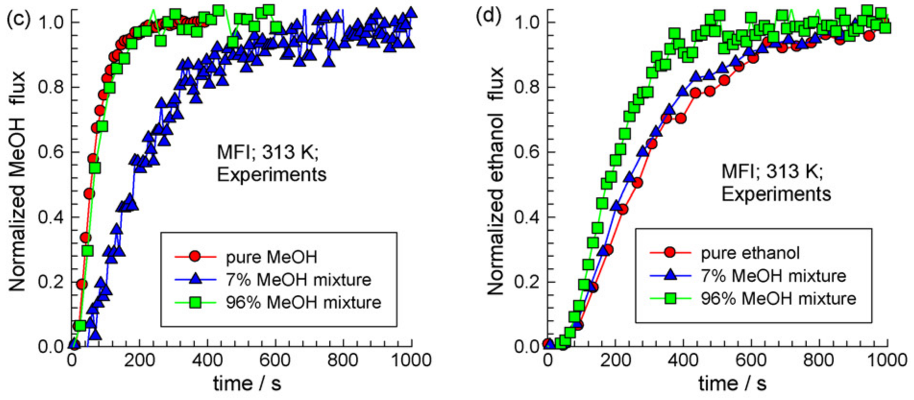

Methanol – acetone mixtures

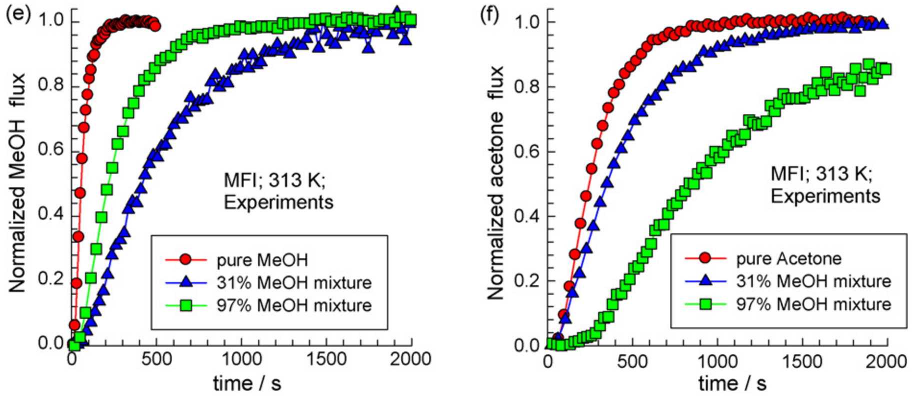

Fig. 1. Experimentally determined transient permeation fluxes for mixtures of (a and b) methanol–2-propanol, (c and d) methanol–ethanol, and (e and f) methanol–acetone.

$Đ_i$ was suggested:

$$Đ_{ij} = [Đ_i]^{q_i/(q_i+q_j)}[Đ_j]^{q_j/(q_i+q_j)} \quad (4)$$

Eq. (4) represents an extension to zeolite diffusion of the interpolation formula that was suggested by Vignes for diffusion in liquid mixtures [25]. Eq. (4) has been widely used in practice for modeling mixture permeation across zeolite membranes [26–28]. More recent work using MD simulations [29–32] has shown unequal saturation capacities violates the symmetry assumption of the $Đ_{ij}$; conformity with the Onsager Reciprocal Relations demands that

$$q_{j,\mathrm{sat}}Đ_{ij} = q_{i,\mathrm{sat}}Đ_{ji} \quad (5)$$

Furthermore, the following, more general, interpolation formula has shown to be valid for mixture diffusion in zeolites and carbon nanotubes [29–33]:

$$q_{j,\mathrm{sat}}Đ_{ij} = [q_{j,\mathrm{sat}}Đ_{ii}]^{q_i/(q_i+q_j)}[q_{i,sat}Đ_{jj}]^{q_j/(q_i+q_j)} = q_{i,\mathrm{sat}}Đ_{ji} \quad (6)$$

where $Đ_{ii}$ is the *self*-exchange coefficient. The Vignes interpolation formula (4) is recovered from Eq. (6) when $q_{j,\mathrm{sat}} = q_{i,\mathrm{sat}}$ and $Đ_{ii}/Đ_i = 1$ for all species. MD simulation results for alkane mixtures in MFI, FAU, and MOR have shown that $Đ_{ii}/Đ_i$ can be significantly smaller than unity, especially for high occupancies [30,31]. This would suggest that slowing-down and speeding-up processes are stronger than anticipated by the Vignes formula (4) for MFI, FAU, and MOR.

In order to model the mixture transients, published MD simulation results for the loading dependence was used as a guideline [34], and the M–S diffusivities of each component was assumed to decrease linearly with total occupancy following:

$$Đ_i = Đ_i(0)(1-\theta) \quad (7)$$

The zero-loading diffusivities $Đ_i(0)$ were chosen to match the pure component transient permeation data.

The primary objective of this paper is to examine the extent to which Eq. (1) is successful in modeling mixture permeation. In particular we aim to show that the mutual influence of the species in the mixture can be much stronger than hitherto appreciated in the literature [35]. Furthermore we aim to show that for methanol/acetone mixtures the assumption that the $Đ_i$ in Eq. (1) can be identified with the pure component diffusivities is open to question.

4. Results and discussion

4.1. Membrane characterization

The XRD pattern of the zeolite crystals collected during membrane M1 synthesis corresponded to the MFI structure with

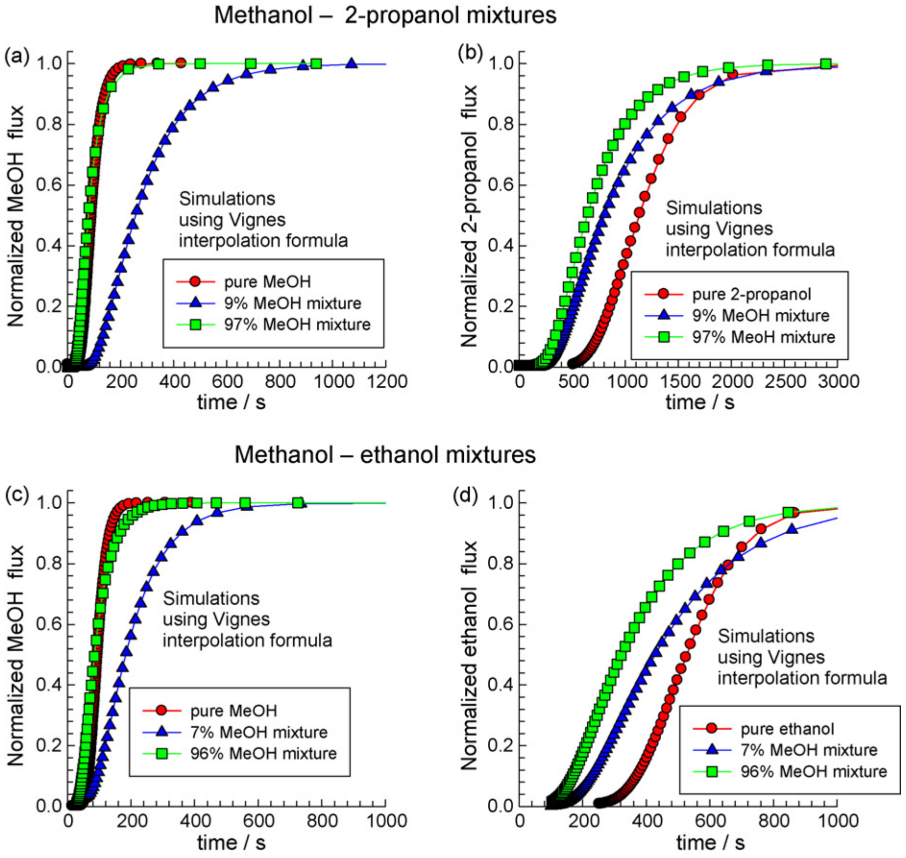

Fig. 2. Simulation results for transient permeation for (a and b) methanol–2-propanol, and (c and d) methanol–ethanol mixtures obtained using the Vignes interpolation formula (4) for estimation of $Đ_{12}$. In these simulations $\rho = 1796\,\mathrm{kg\,m^{-3}}$; $\delta = 30\,\mu\mathrm{m}$; $Đ_{\mathrm{methanol}}(0) = 5\times10^{-11}\,\mathrm{m^2\,s^{-1}}$; $Đ_{\text{2-propanol}}(0) = 4\times10^{-12}\,\mathrm{m^2\,s^{-1}}$; $Đ_{\mathrm{ethanol}}(0) = 9\times10^{-12}\,\mathrm{m^2\,s^{-1}}$.

high crystallinity. A SEM of membrane M2, which was prepared by the same method as M1, showed a ∼30 μm thick continuous zeolite layer, and EPMA yielded a Si/Ge ratio of 41 [2]. At 473 K, the n-/i-C_4H_{10} ideal permselectivity for membrane M1 were 5, and the n-/i-C_4H_{10} mixture selectivity was 19 at 373 K. Both n-C_4H_{10} and i-C_4H_{10} mixture permeances increased with temperature, and the n-C_4H_{10} permeance was 1.7×10^{-8} mol/m^2 s Pa at 473 K. These selectivities are comparable n-/i-C_4H_{10} selectivities reported in the literature for MFI membranes: 24 at 473 K [36], 11 at 408 K [37], and 3 at 433 K [38]. Membrane M1 had an ethanol/water separation factor during pervaporation of 54, with a flux of 4.4 mol/m^2 h (122 g/m^2 h) at 313 K. This selectivity is also similar to literature values for MFI membranes; ethanol/water selectivities of 47 at 303 K [39], 72 at 333 K [40], 106 at 333 K [6], and 70 at 303 K [41] have been reported. Thus membranes M1 and M2 have similar separation properties to MFI membranes reported previously.

4.2. Modeling of transient mixture permeation

The normalized permeation fluxes of methanol and 2-propanol, both for pure components and in 9 mol%, and 97 mol% methanol/2-propanol mixtures are shown in Fig. 1a and b. Fig. 1a shows that the more-mobile methanol is slowed down considerably when the mixture contains 91% of the tardy 2-propanol. Note in Fig. 1b that the relatively sluggish 2-propanol speeds up significantly in a mixture containing 97% of the more-mobile methanol. For the 9% methanol mixture, methanol has almost no influence on the permeation flux of 2-propanol. A similar picture emerges for the permeation of mixtures of methanol and ethanol; see Fig. 1c and d. Adding 93% ethanol tends to slow down methanol considerably (Fig. 1c), whereas adding 96% methanol significantly speeds up the tardier ethanol (Fig. 1d). The permeation results for methanol/acetone mixtures, presented in Fig. 1e and f, are different from the foregoing in that both methanol and acetone are slowed in the mixtures containing 31% and 97% methanol.

For simulation of the transient permeation experiments a rigorous numerical solution of the M–S equation (1), as described in earlier work [23,42] was employed. The pure component isotherm literature data [43–45], available at 298 K, along with data on heats of adsorption [17] were used to estimate the single site Langmuir parameters at a temperature of 313 K at which the experiments were carried out; the parameters are listed in Table 1. The ideal adsorbed solution theory (IAST) of Myers and Prausnitz [46] was used to estimate the component loadings in the mixture.

Consider first the modeling of the methanol/2-propanol permeation using the Vignes interpolation formula (4); the results are shown in Fig. 2a and b. Fitted $Đ_i(0)$ values are specified in the legend to Fig. 2. Comparison of Figs. 1a and 2a shows

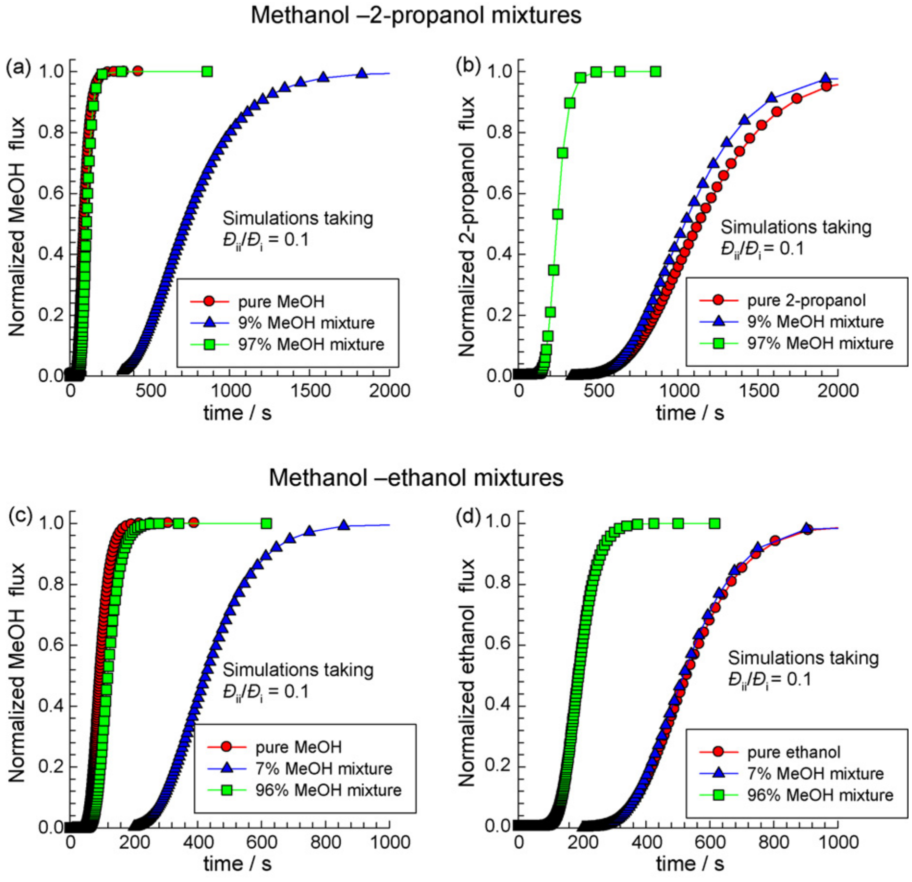

Fig. 3. Simulation results for transient permeation for (a and b) methanol–2-propanol, and (c and d) methanol–ethanol mixtures obtained using the interpolation formula (6) taking $Đ_{ii}/Đ_i = 0.1$ for each component. Other parameter values are as specified in the legend to Fig. 2.

Table 1
Pure component isotherm data using single-site Langmuir model

Molecule	b_i (Pa^{-1})	$q_{i,\mathrm{sat}}$ ($\mathrm{mol\,kg}^{-1}$)
Methanol	3.5×10^{-4}	3.8
2-Propanol	3×10^{-4}	2.3
Ethanol	6.9×10^{-4}	3
Acetone	1.8×10^{-2}	2

that the slowing down effect on methanol in the 9% mixture is much more severe in the experiments than anticipated by the Vignes formula (4). Concomitantly, the experiments for this 9% mixture shows no speeding up of 2-propanol; whereas the Vignes formula (4) predicts a sizable speeding up even with this low concentration of methanol present in the mixture; compare Figs. 1b and 2b. Perversely, for the 97% methanol mixture the speeding up of 2-propanol is much *more significant* than predicted.

An entirely analogous picture emerges for simulations of the methanol–ethanol permeation experiments with the Vignes formula (4). The simulations show much smaller slowing down of methanol than in the experiments with the 7% mixture. Also, the predicted speeding up of ethanol in the 7% mixture is almost non-existent in the experiments.

Use of the more general interpolation formula (6) taking the values of $Đ_{ii}/Đ_i = 0.1$ are shown in Fig. 3; this leads to a much closer agreement of the simulations with the experiments. The slowing down of methanol is much more significant as compared to the simulations with the Vignes formula (4). For 2-propanol there is considerable speeding up for the 97% methanol mixture, while for the 9% mixture the speeding up process is predicted to be negligible; this is entirely in agreement with the experiments. For the methanol/ethanol mixtures too, considerably better agreement between experiments and simulations is obtained by taking $Đ_{ii}/Đ_i = 0.1$.

Simulation of the methanol–acetone mixture experimental results within the framework of the M–S equations is not possible even by adjusting the ratio $Đ_{ii}/Đ_i$; the results will always predict a speeding up of acetone, with concomitant slowing down of methanol. Within the M–S framework the only possibility of predicting slowing down of both components is to allow the M–S diffusivities $Đ_i$ in the mixture to be lower than the values of the corresponding pure components.

5. Conclusions

Transient permeation experiments with methanol/2-propanol, methanol/ethanol, and methanol/acetone mixtures across MFI membranes have led to the following conclusions:

(1) The experimental results for permeation of methanol/2-propanol and methanol/ethanol indicate that the self-exchange coefficient $Đ_{ii}$ is about a tenth of the value of the pure component M–S diffusivity $Đ_i$. This suggests much stronger mixture correlation for polar mixtures through MFI zeolite membranes.

(2) The experimental results for permeation of methanol/acetone mixtures show that *both* components are slowed down. These results are not amenable to modeling the M–S formulation unless we allow for significantly lower $Đ_i$ values for either species in the mixture than for the pure components.

Acknowledgments

We gratefully acknowledge the support from National Science Foundation Grant CTS-0340563. MY also acknowledges a fellowship from the U.S. Department of Education Graduate Assistantship in Areas of National Need (GAANN) program. We thank Dr. Vu A. Tuan for preparing the membranes.

Nomenclature

b_i	pure component adsorption constant (Pa^{-1})
$Đ_i$	single component Maxwell–Stefan diffusivity of species *i* (m^2/s)
$Đ_{ii}$	Maxwell–Stefan diffusivity representing interchange between species *i* and species *j* (m^2/s)
n	total number of diffusing species
N_i	flux of species *i* ($\mathrm{mol\,m}^{-2}\,\mathrm{s}^{-1}$)
q_i	loading of species *i* in mixture ($\mathrm{mol\,kg}^{-1}$)
$q_{i,\mathrm{sat}}$	saturation loading of species *i* ($\mathrm{mol\,kg}^{-1}$)
R	gas constant
T	absolute temperature (K)

Greek letters

ρ	zeolite framework density ($\mathrm{kg\,m}^{-3}$)
θ	total fractional loading
θ_i	fractional occupancy of component *i*
δ	membrane thickness (μm)

References

[1] J.R. Xiao, J. Wei, Diffusion mechanism of hydrocarbons in zeolites. 1. Theory, Chem. Eng. Sci. 47 (1992) 1123.

[2] S. Li, V.A. Tuan, J.L. Falconer, R.D. Noble, Properties and separation performance of Ge-ZSM-5 membranes, Micropor. Mesopor. Mater. 58 (2003) 137.

[3] S.G. Li, V.A. Tuan, R.D. Noble, J.L. Falconer, Pervaporation of water/THF mixtures using zeolite membranes, Ind. Eng. Chem. Res. 40 (2001) 4577.

[4] Z.P. Lai, G. Bonilla, I. Diaz, J.G. Nery, K. Sujaoti, M.A. Amat, E. Kokkoli, O. Terasaki, R.W. Thompson, M. Tsapatsis, D.G. Vlachos, Microstructural optimization of a zeolite membrane for organic vapor separation, Science 300 (2003) 456.

[5] M. Kazemimoghadam, A. Pak, T. Mohammadi, Dehydration of water/1-1-dimethylhydrazine mixtures by zeolite membranes, Micropor. Mesopor. Mater. 70 (2004) 127.

[6] X. Lin, X.S. Chen, H. Kita, K. Okamoto, Synthesis of silicalite tubular membranes by in situ crystallization, AIChE J. 49 (2003) 237.

[7] N. Nishiyama, K. Ueyama, M. Matsukata, Synthesis of defect-free zeolite-alumina composite membranes by a vapor-phase transport method, Micropor. Mater. 7 (1996) 299.

[8] K. Okamoto, H. Kita, K. Horii, K. Tanaka, M. Kondo, Zeolite NaA membrane: preparation, single-gas permeation, and pervaporation and vapor

permeation of water/organic liquid mixtures, Ind. Eng. Chem. Res. 40 (2001) 163.

[9] B.H. Jeong, Y. Hasegawa, K.I. Sotowa, K. Kusakabe, S. Morooka, Permeation of binary mixtures of benzene and saturated C_4–C_7 hydrocarbons through an FAU-type zeolite membrane, J. Membr. Sci. 213 (2003) 115.

[10] S. Jost, N.K. Bar, S. Fritzsche, R. Haberlandt, J. Karger, Diffusion of a mixture of methane and xenon in silicalite: a molecular dynamics study and pulsed field gradient nuclear magnetic resonance experiments, J. Phys. Chem. B 102 (1998) 6375.

[11] R. Krishna, D. Paschek, Self-diffusivities in multicomponent mixtures in zeolites, Phys. Chem. Chem. Phys. 4 (2002) 1891.

[12] R.Q. Snurr, J. Karger, Molecular simulations and NMR measurements of binary diffusion in zeolites, J. Phys. Chem. B 101 (1997) 6469.

[13] D. Paschek, R. Krishna, Diffusion of binary mixtures in zeolites: kinetic Monte Carlo versus molecular dynamics simulations, Langmuir 17 (2001) 247.

[14] T. Masuda, Y. Fujiikata, H. Ikeda, K. Hashimoto, Diffusivities in the binary components system within MFI-type zeolite crystals, Micropor. Mesopor. Mater. 38 (2000) 323.

[15] J. Du Plessis, W.J. Pugh, A. Judefeind, J. Hadgraft, The effect of the nature of H-bonding groups on diffusion through PDMS membranes saturated with octanol and toluene, Eur. J. Pharm. Sci. 15 (2002) 63.

[16] Y.A. Elabd, T.A. Barbari, Multicomponent diffusion of hydrogen-bonding solutes in a polymer, AIChE J. 48 (2002) 1610.

[17] T.C. Bowen, J.C. Wyss, R.D. Noble, J.L. Falconer, Measurements of diffusion through a zeolite membrane using isotopic-transient pervaporation, Micropor. Mesopor. Mater. 71 (2004) 199.

[18] T.C. Bowen, J.C. Wyss, R.D. Noble, J.L. Falconer, Inhibition during multicomponent diffusion through ZSM-5 zeolite, Ind. Eng. Chem. Res. 43 (2004) 2598.

[19] T. Gallego-Lizon, E. Edwards, G. Lobiundo, L.F. dos, Santos, Dehydration of water/*t*-butanol mixtures by pervaporation: comparative study of commercially available polymeric, microporous silica and zeolite membranes, J. Membr. Sci. 197 (2002) 309.

[20] J.F. Smetana, J.L. Falconer, R.D. Noble, Separation of methyl ethyl ketone from water by pervaporation using a silicalite membrane, J. Membr. Sci. 114 (1996) 127.

[21] Q. Liu, R.D. Noble, J.L. Falconer, H.H. Funke, Organics/water separation by pervaporation with a zeolite membrane, J. Membr. Sci. 117 (1996) 163.

[22] F. Kapteijn, J.A. Moulijn, R. Krishna, The generalized Maxwell–Stefan model for diffusion in zeolites: sorbate molecules with different saturation loadings, Chem. Eng. Sci. 55 (2000) 2923.

[23] R. Krishna, R. Baur, Modelling issues in zeolite based separation processes, Sep. Purif. Technol. 33 (2003) 213.

[24] J.V.S. Kärger, S.M. Auerbach, in: S.M. Auerbach, K.A. Carrado, P.K. Dutta (Eds.), Diffusion in zeolites, Chapter 10. In Handbook of Zeolite Science and Technology, Marcel Dekker, New York, 2003, pp. 341–422.

[25] A. Vignes, Diffusion in binary solutions—variation of diffusion coefficient with composition, Ind. Eng. Chem. Fund. 5 (1966) 189.

[26] W.D. Zhu, P. Hrabanek, L. Gora, F. Kapteijn, J.A. Moulijn, Role of adsorption in the permeation of CH_4 and CO_2 through a silicalite-1 membrane, Ind. Eng. Chem. Res. 45 (2006) 767.

[27] S.G. Li, J.G. Martinek, J.L. Falconer, R.D. Noble, T.Q. Gardner, High-pressure CO_2/CH_4 separation using SAPO-34 membranes, Ind. Eng. Chem. Res. 44 (2005) 3220.

[28] A. Salem, A.A. Ghoreyshi, M. Jahanshahi, A multicomponent transport model for dehydration of organic vapors by zeolite membranes, Desalination 193 (2006) 35.

[29] A.I. Skoulidas, D.S. Sholl, R. Krishna, Correlation effects in diffusion of CH4/CF4 mixtures in MFI zeolite. A study linking MD simulations with the Maxwell–Stefan formulation, Langmuir 19 (2003) 7977.

[30] R. Krishna, J.M. van Baten, Diffusion of alkane mixtures in zeolites: validating the Maxwell–Stefan formulation using MD simulations, J. Phys. Chem. B 109 (2005) 6386.

[31] J.M. van Baten, R. Krishna, Entropy effects in adsorption and diffusion of alkane isomers in mordenite: an investigation using CBMC and MD simulations, Micropor. Mesopor. Mater. 84 (2005) 179.

[32] R. Krishna, J.M. van Baten, Describing binary mixture diffusion in carbon nanotubes with the Maxwell–Stefan equations. An investigation using molecular dynamics simulations, Ind. Eng. Chem. Res. 45 (2006) 2084.

[33] S. Chempath, R. Krishna, R.Q. Snurr, Nonequilibrium molecular dynamics simulations of diffusion of binary mixtures containing short *n*-alkanes in faujasite, J. Phys. Chem. B 108 (2004) 13481.

[34] R. Krishna, J.M. van Baten, Linking the loading dependence of the Maxwell–Stefan diffusivity of linear alkanes in zeolites with the thermodynamic correction factor, Chem. Phys. Lett. 420 (2006) 545.

[35] M. Yang, B.D. Crittenden, S.P. Perera, H. Moueddeb, J.A. Dalmon, The hindering effect of adsorbed components on the permeation of a non-adsorbing component through a microporous silicalite membrane: the potential barrier theory, J. Membr. Sci. 156 (1999) 1.

[36] K. Keizer, A.J. Burggraaf, Z.A.E.P. Vroon, H. Verweij, Two component permeation through thin zeolite MFI membranes, J. Membr. Sci. 147 (1998) 159.

[37] J. Coronas, R.D. Noble, J.L. Falconer, Separations of C-4 and C-6 isomers in ZSM-5 tubular membranes, Ind. Eng. Chem. Res. 37 (1998) 166.

[38] J. Hedlund, J. Sterte, M. Anthonis, A.J. Bons, B. Carstensen, N. Corcoran, D. Cox, H. Deckman, W. De Gijnst, P.P. de Moor, F. Lai, J. McHenry, W. Mortier, J. Reinoso, High-flux MFI membranes, Micropor. Mesopor. Mater. 52 (2002) 179.

[39] T.C. Bowen, S.G. Li, R.D. Noble, J.L. Falconer, Driving force for pervaporation through zeolite membranes, J. Membr. Sci. 225 (2003) 165.

[40] X. Lin, H. Kita, K. Okamoto, A novel method for the synthesis of high performance silicalite membranes, Chem. Commun. (2000) 1889.

[41] H. Matsuda, H. Yanagishita, D. Kitamoto, K. Haraya, T. Nakane, T. Takada, Y. Idemoto, N. Koura, T. Sano, Preparation of silicalite pervaporation membrane with ethanol permselectivity by a 2-step hydrothermal synthesis, Separ. Sci. Technol. 36 (2001) 3305.

[42] R. Krishna, R. Baur, Diffusion, Adsorption and Reaction in Zeolites: Modelling and Numerical Issues, University of Amsterdam, Amsterdam, 2004, http://www.science.uva.nl/research/cr/zeolite/.

[43] V.S. Nayak, J.B. Moffat, Sorption and diffusion of alcohols in heteropoly oxometalates and Zsm-5 zeolite, J. Phys. Chem. 92 (1988) 7097.

[44] T.C. Bowen, L.M. Vane, Ethanol acetic acid, and water adsorption from binary and ternary liquid mixtures on high-silica zeolites, Langmuir 22 (2006) 3721.

[45] T.C. Bowen, R.D. Noble, J.L. Falconer, Fundamentals and applications of pervaporation through zeolite membranes, J. Membr. Sci. 245 (2004) 1.

[46] A.L. Myers, J. Prausnitz, Thermodynamics of mixed-gas adsorption, AIChE J. 11 (1965) 121.